journal of the mechanical behavior of biomedical materials 127 (2022) 105057

Contents lists available at ScienceDirect

Journal of the Mechanical Behavior of Biomedical Materials

journal homepage: www.elsevier.com/locate/jmbbm

Tensile fatigue strength and endurance limit of human meniscus

Bradley S. Henderson, Katelyn F. Cudworth, Madison E. Wale, Danielle N. Siegel, Trevor J. Lujan *

Department of Mechanical & Biomedical Engineering, Boise State University, Boise, ID, USA

ARTICLE INFO

Keywords:
Fatigue life
Soft tissue
Effect of Aging
Mechanical properties
Damage
Probability of Fatigue Failure

ABSTRACT

The knee menisci are prone to mechanical fatigue injury from the cyclic tensile stresses that are generated during daily joint loading. Here we characterize the tensile fatigue behavior of human medial meniscus and investigate the effect of aging on fatigue strength. Test specimens were excised from the medial meniscus of young (under 40 years) and older (over 65 years) fresh-frozen cadaver knees. Cyclic uniaxial tensile loads were applied parallel to the primary circumferential fibers at 70%, 50%, 40%, or 30% of the predicted ultimate tensile strength (UTS) until failure occurred or one million cycles was reached. Equations for fatigue strength (S-N curve) and the probability of fatigue failure (unreliability curves) were created from the measured number of cycles to failure. The mean number of cycles to failure at 70%, 50%, 40%, and 30% of UTS were estimated to be approximately 500, 40000, 340000, and 3 million cycles, respectively. The endurance limit, defined as the tensile stress that can be safely applied for the average lifetime of use (250 million cycles), was estimated to be 10% of UTS (~1.0 MPa). When cyclic tensile stresses exceeded 30% of UTS (~3.0 MPa), the probability of fatigue failure rapidly increased. While older menisci were generally weaker and more susceptible to fatigue failures at high-magnitude tensile stresses, both young and older age groups had similar fatigue resistance at low-magnitude tensile stresses. In addition, we found that fatigue failures occurred after the dynamic modulus decreased during cyclic loading by approximately 20%. This experimental study has quantified fundamental fatigue properties that are essential to properly predict and prevent injury in meniscus and other soft fibrous tissues.

1. Introduction

Acute meniscal tears are a common injury in the adult human knee, with a prevalence of 12–14% in the United States (Majewski et al., 2006; Stocker et al., 1997). These tears disrupt the functional capacity of the meniscus to facilitate smooth articulations and distribute loads across the tibiofemoral joint (Fox et al., 2012). Consequently, meniscal tears result in pain, joint instability, and an increased risk of osteoarthritis to the tibiofemoral articular surfaces (Ding et al., 2007). While the majority of acute meniscal tears occur from a single high-magnitude load, a third of patients may experience an acute tear without a traumatic event (Camanho et al., 2006). These atraumatic tears suggest a fatigue injury, where repeated exposure to low-magnitude cyclic loads lead to an accumulation of damage and eventual rupture of the fibrous tissue. The anisotropic fiber network of the fibrocartilagenous meniscus is primarily aligned circumferentially to resist the tensile or hoop stresses that develop in the semi-circular meniscus during joint compression (Fox et al., 2012), and therefore meniscal tissue is subjected to millions of low-magnitude tensile loads during an individual's lifetime. The prevention and treatment of meniscal injuries caused by repeated joint loading requires the material characterization of fatigue behavior, yet no study has measured the fatigue properties of human meniscus.

A fundamental fatigue property is fatigue strength, which corresponds to the stress level where a material will fail at a specific number of cycles. The fatigue strength is called the fatigue limit (or endurance limit) when the number of cycles reached has exceeded the number of cycles the material is expected to withstand in its lifetime (ASTM, 2017). Fatigue strengths are frequently used to determine safe loading limits for specific materials, designs, and loading configurations (Budynas and Nisbett, 2014), and the relationship between fatigue strength and cycles to failure (S-N curve) has been experimentally characterized for most standard metals (Fatemi, 2000), plastics (McKeen, 2009), and composites (Harris, 2003) by applying thousands to millions of loading cycles (high-cycle testing) to sectioned specimen coupons that are representative of the bulk material. In biological materials, fatigue strengths are largely unknown, with only a few studies developing S-N curves for soft

* Corresponding author. 1910 University Drive Boise, ID, 83725-2085, USA.
E-mail address: trevorlujan@boisestate.edu (T.J. Lujan).

https://doi.org/10.1016/j.jmbbm.2021.105057
Received 31 July 2021; Received in revised form 6 December 2021; Accepted 17 December 2021
Available online 6 January 2022

fibrous tissues (Sadeghi et al., 2017; Schechtman and Bader, 1997; Scholze et al., 2018). Fatigue studies in soft and hard tissue are typically conducted at randomized stress levels; however, international test standards recommend the fatigue testing of multiple specimens at targeted stress levels (ASTM, 2017). One advantage of this standardized approach is that unreliability equations can be readily developed to estimate the risk of material failure for a given stress and number of cycles. To our knowledge, S-N curves have not been reported for human meniscus, and unreliability equations and tensile endurance limits have not been reported for any biological soft tissue. Quantifying these fatigue behaviors can allow research groups that calculate tissue stresses in knee joints using in-vivo, in-vitro, and in-silico approaches (Yao et al., 2006) to assess the relative risk (or safety) of specific physiological joint loads.

A material's fatigue strength and endurance limit can be altered by intrinsic and extrinsic factors called modifying factors (Budynas and Nisbett, 2014). In manufactured materials, modifying factors include fabrication method, operating temperature, and material composition. In biological materials, a potential modifying factor for fatigue behavior is specimen age. Aging can alter the composition and organization of the extracellular matrix (Kempson, 1982; Tsujii et al., 2017), and age-related reductions in tissue extensibility and energy to failure in human meniscus have been observed in uniaxial pull-to-failure experiments (Nesbitt et al., 2021). Age-related structural changes may likewise make meniscus more susceptible to fatigue injuries, and may contribute to the high prevalence (>50%) of meniscal tears and degeneration in individuals over the age of 70 years (Englund et al., 2008).

The objective of this study is to characterize the high-cycle tensile fatigue behavior of human meniscus. We hypothesize that specimens from donors over 65 years will have reduced fatigue strength compared to specimens from donors under 40 years.

2. Materials and methods

2.1. Overview

Young and older human medial meniscus specimens were repeatedly loaded at four stress levels (70%, 50%, 40%, or 30% of their predicted UTS) until failure or one million cycles was reached. Plots of stress level vs. cycles to failure were generated to estimate fatigue strength and the endurance limit, and the probability of failure at each stress level for a given number of cycles was determined using cumulative distribution functions. The creep curves were analyzed to calculate fatigue properties (creep rate, damage rate, and failure strain), as well as the elongation and number of cycles at different stages of cyclic creep. In addition, monotonic pull to failure experiments were conducted to measure static mechanical properties for specimens that were not fatigue tested, and for specimens that were fatigue tested but did not fail before one million cycles (run-outs).

2.2. Specimen preparation

Medial menisci were obtained from eleven unpaired human fresh frozen cadaveric knee joints (femur to tibia), with six knees from "young" donors between 18 and 40 (age = 31 ± 7 years; 4 male and 2 female), and five knees from "older" donors over the age of 65 (age = 72 ± 7 years; 4 male and 1 female). The rationale for these age groups is that meniscus tensile properties don't have noticeable changes before 40 years (Bursac et al., 2009), while above 65 years, the meniscus has reduced extensibility and toughness (Nesbitt et al., 2021) and a high incidence of damage (Loeser, 2010). All knees used for this study had no medical history of injury and showed no sign of arthritis. Knee joints were stored at -20 °C and were allowed to thaw at room temperature for at least 24 h prior to dissection. Menisci were harvested, sectioned into anterior and posterior regions (Fischenich et al., 2015), packed in CelluClay (Actíva, Marshall TX), and frozen for at least 24 h prior to being layered along the circumferential-axial plane into ~0.9 mm thick specimens using a commercial deli slicer (Wale et al., 2021). This resulted in 8 anterior and 8 posterior layers that were useable for mechanical testing. After layering, specimens were cut into dumbbell-shaped coupons (Fig. 1A and B) by aligning the long-axis of a custom punch (Nelson et al., 2020) along the circumferential fiber direction. A 5:1 aspect ratio for the gauge section was selected to reduce the incidence of grip failures (Wale et al., 2021). The mean fiber orientation of the tensile coupons relative to the loading axis (Table 1) was quantified by analyzing light microscopy images (Fig. 1C) with FiberFit software (Fig. 1D) (Morrill et al., 2016). In total, 32 specimens were cyclically tested and analyzed to characterize tensile fatigue behavior, and 16 additional specimens were monotonically tested and analyzed to measure tensile strength and stiffness.

2.3. Fatigue testing

Material fatigue was characterized in human medial meniscus using the stress-life method. This test method measures the number of cycles to failure at specific fatigue strengths (targeted stress levels) below a material's ultimate tensile strength (UTS), where the fatigue strength can be represented as a percentage of UTS (%UTS). Applying this test method to highly heterogeneous materials like soft fibrous tissue is intrinsically challenging, since large intra- and inter-specimen variations exist when measuring the UTS. This large variability negates the reliable use of an average UTS value when prescribing the maximum cyclic stress (%UTS) during fatigue testing for a specific meniscus specimen. Our previous work with bovine meniscus found that the specimen-specific UTS could be reliably predicted by first conducting a series of monotonic tensile experiments to failure to calculate the linear correlation between UTS and linear modulus. This correlation could then provide a non-destructive method to predict the UTS for fatigue specimens via the measurement of linear modulus prior to fatigue testing (Creechley et al., 2017). The present study replicated this methodology by first conducting monotonic tensile experiments to failure on eight young and eight older dumbbell-shaped human medial meniscus specimens that were taken from the same set of menisci used for fatigue testing. Linear correlations were created for both the young group ($R^2 = 0.89$) and the older group ($R^2 = 0.76$), and these correlations were used to estimate the UTS of the fatigue specimens prior to cyclic loading. A detailed description of the test methods used for monotonic testing can be found in the Supplementary Data.

Fatigue experiments were conducted using an electrodynamic test system (Instron, Norwood MA; ElectroPuls E10000) equipped with an acrylic immersion chamber (Test Resources, Shakopee MN; T200 Bath Controller) (Fig. 1E). Prior to inserting coupons into the test grips, the rough surface of emery cloth tabs were bonded to each end of the specimen with cyanoacrylate to reduce slipping at the grips (Fig. 1F) (Wale et al., 2021). Specimens were mounted in the mechanical testing system and preloaded to 0.1 N. At this position, front and side profile images were taken with a digital camera to measure the initial cross-sectional area (Creechley et al., 2017) (Table 1). The specimen was then buckled and the immersion tank was filled with 37 °C saline solution containing 0.05 mg/mL of both penicillin and streptomycin. The addition of penicillin and streptomycin inhibited bacterial cell growth during the multiple-day fatigue tests. The solution was kept at 37 °C (±1 °C) to mimic normal body temperature, and the specimen was allowed to equilibrate in the heated bath for 1.5 h. After this equilibration period, the sample was again preloaded to 0.1 N, then preconditioned with a 20 cycle triangular wave at 2 Hz to 8% clamp strain. The linear modulus was determined via the 20th preconditioning cycle by applying a linear fit between strain values of 6.5 and 7.5 percent. As mentioned previously, the specimen-specific UTS was then predicted from this linear modulus by using the linear regression function of UTS vs. linear modulus, acquired from monotonic experiments to failure (see Supplementary Data). Each specimen's predicted UTS was used to

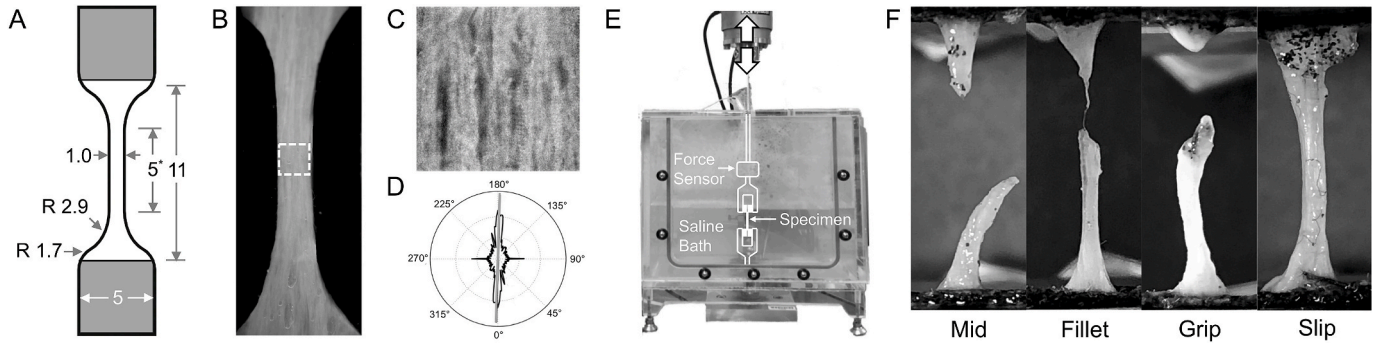

Fig. 1. Tensile testing of human medial meniscus specimens. A) Dimensions of the punch used to cut dumbbell-shaped coupons from thin layers of meniscus. B) The central region of the gauge section (white dashed square) was C) imaged using a light microscope, and D) analyzed for fiber orientation using FiberFit software. E) Coupon specimens were inserted into a saline tank heated to 37 °C. For fatigue testing, specimens were preconditioned and cycled in tension (white arrows) until failure. F) Mechanical failure was characterized as midsubstance, fillet, grip, or slip. All grip and slip failures occurring during fatigue testing were discarded and excluded from further analysis.

Table 1
Physical characteristics of all medial meniscus test specimens used for fatigue testing.

Stress Level (%UTS)	Width[a] (mm)	Thickness[a] (mm)	Cross-Sectional Area[a] (mm^2)	Grip-to-Grip Length (mm)	Mean Fiber Orientation[b] (deg)
70	1.05 ± 0.11	0.85 ± 0.15	0.89 ± 0.14	10.16 ± 0.29	2.6 ± 3.3
50	1.01 ± 0.10	0.95 ± 0.21	0.98 ± 0.30	10.55 ± 0.56	9.0 ± 15.3
40	1.05 ± 0.06	0.93 ± 0.20	0.98 ± 0.24	9.84 ± 0.48	4.0 ± 5.2
30	0.98 ± 0.11	0.86 ± 0.23	0.84 ± 0.24	10.17 ± 0.51	3.6 ± 3.3
Total	1.02 ± 0.10	0.90 ± 0.20	0.92 ± 0.23	10.18 ± 0.52	4.8 ± 8.4

[a] Measured in the gauge section.
[b] Measured relative to the loading axis.

calculate the targeted maximum tensile stress at a specific %UTS (70%, 50%, 40%, or 30%). After preconditioning, the sample was again preloaded to 0.1 N, and the reference specimen length was established from the grip-to-grip displacement after this preload.

Specimens were fatigued using a 4 Hz tension-tension sine wave that was applied to the targeted maximum tensile stress (after converting to force), where the targeted minimum tensile stress was 10% of the maximum tensile stress. Force and displacement data were converted to engineering stress (Fig. 2A) and engineering strain (Fig. 2B) using the reference area and length (Wale et al., 2021). The targeted maximum tensile stress was successfully maintained throughout fatigue testing (average absolute error = 1.7% ± 1.4%) until specimen failure or one million cycles was reached. Specimens that did not fail after one million cycles were considered run-outs, and were pulled to failure to measure the failure strain at UTS (see Supplementary Data for details). Failure type was classified for each specimen that failed before one million cycles (mid = 10, fillet = 11, grip = 9, slip = 4) and for each run-out specimen that was pulled to failure after one million cycles of fatigue testing (mid = 3, fillet = 6, grip = 2, slip = 2) (Fig. 1F). Fatigue specimens that failed at the grips before one million cycles, and specimens that slipped during either fatigue testing or UTS testing for the run-outs, were discarded and excluded from further analysis. In total, 32 specimens were analyzed for fatigue behavior, with two-thirds of those specimens failing before one million cycles.

2.4. Analysis of fatigue behavior

After mechanical testing, the experimental data was analyzed to calculate material properties of interest. The number of cycles to failure was calculated by subtracting the start cycle from the tear cycle (Fig. 2C). The start cycle was defined as the first cycle during the initial ramping period to have a maximum tensile stress greater than 75% of the target tensile stress, and once the targeted stress was achieved, the end cycle was defined as the first cycle to not maintain at least 95% of the target tensile stress (Fig. 2C). The ultimate strain for the specimens that failed during fatigue testing was calculated using the maximum strain at the tear cycle (Fig. 2D). In addition, the cyclic creep behavior was split into three characteristic stages (Fig. 3A) (Shepherd and Screen, 2013). Stage I exhibits a rapid increase in strain over a short cycle period until stage II, where cyclic creep stabilizes over a long cycle period. In stage III, cyclic creep becomes unstable and rapidly increases until material rupture. The transitions between these stages were automatically identified using a custom MATLAB algorithm. This program first applied a polynomial fit and smoothed the experimental cyclic creep curve data, and then picked the absolute minimum second derivative (closest to zero), a local flex point, which occurred within Stage II (Fig. 3A). The transitions between stages were marked by a 10% increase in the absolute minimum second derivative, in both directions, from the local flex point (Fig. 3A). The rate of cyclic creep, per 1000 cycles, was determined from the slope of the linear fit of data in Stage II (R^2 range of linear fit = 0.94 to 0.99). The damage rate during stage II creep was calculated as the difference in dynamic modulus between the start and end of stage II, divided by the dynamic modulus at the start of stage II. Dynamic modulus was calculated as the ratio of tensile stress amplitude to tensile strain amplitude. At the limits of each stage, the dynamic modulus and specimen elongation (change in length divided by initial reference length) were calculated.

The analysis of specimens that did not fail during fatigue testing (run-outs) required the development of an algorithm, Eq. (1), to predict the number of cycles to failure, also called fatigue life, N_f.

$$N_f = 2N_I + \frac{\Delta\varepsilon}{m} \quad (1)$$

Here, N_I is the number of cycles in Stage I based on experimental data (Fig. 3B), where the specimen-specific transition between Stage I and II was estimated using the same methods described for specimens that experienced fatigue failure. The variable N_I is multiplied by two to also account for the number of cycles that is predicted to occur in stage III.

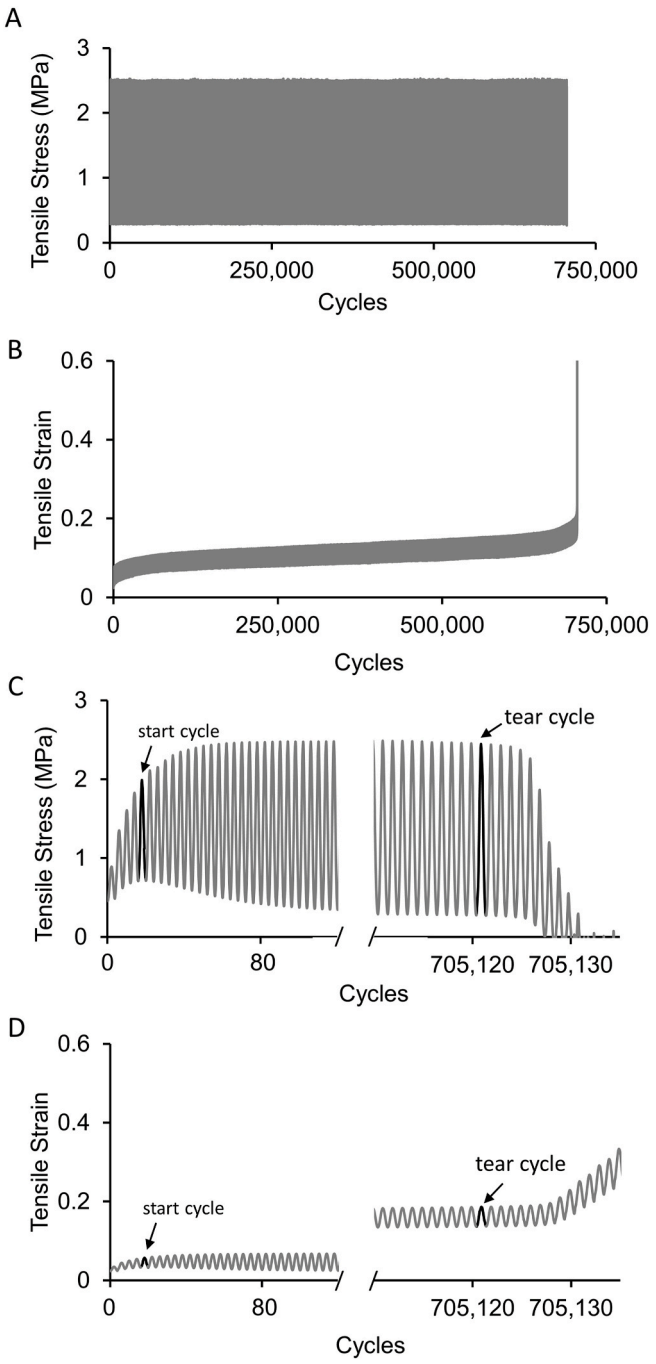

Fig. 2. Stress and strain response during a fatigue experiment. A) A constant cyclic stress amplitude caused B) a steady increase in mean cyclic strain until rupture. C) The targeted maximum and minimum stress was achieved after an initial ramping period of approximately 50–80 cycles. The number of cycles to failure was counted between the start cycle (rises above 75% of targeted stress) and the tear cycle (drops below 95% of targeted stress). The sudden drop in stress after the tear cycle corresponded to D) a rapid increase in mean cyclic strain.

The rationale for using the number of cycles in stage I to predict the number of cycles in stage III, is that when analyzing specimens that experienced fatigue failure, similarity existed in the cyclic durations of stage I (7707 ± 16,857) and stage III (9034 ± 20,472). The second term $\Delta\varepsilon/m$ estimated the number of cycles in Stage II, where the specimen-specific creep rate m is the slope of the linear fit of cyclic creep measured from the start of stage II to one million cycles. The end of stage II was then estimated by extrapolating the creep rate until the net increase in strain, during stage II, exceeded a delta strain value, $\Delta\varepsilon$ (Fig. 3B). In this study, $\Delta\varepsilon$ was estimated by measuring the mean net increase in tensile strain during stage II for all 21 specimens that failed during fatigue testing (0.046 ± 0.025), therefore $\Delta\varepsilon$ was set to 0.046. When using this algorithm, Eq. (1), with experimental data from the 21 specimens with fatigue failures (i.e. the number of cycles to rupture was known) (Fig. 3A), the algorithm generally overpredicted the number of cycles to failure with a median error of 18%.

Diagrams of fatigue strength versus cycles to failure (S-N diagrams) were produced using a three-step process. In the first step, a two-parameter Weibull probability distribution was fit to cycles-to-failure data for each test group using the Matlab function wblfit (Mathworks, Natick, MA). In the second step, the shape and scale parameter for each stress level were used to find the median cycles to failure using the Matlab function wblinv. In the third step, a log-linear function was fit to the median cycles to failure at each stress level to generate an S-N curve. The use of a Weibull probability distribution follows established methods for stress-life fatigue analysis of both human tendon and bovine meniscus (Creechley et al., 2017; Schechtman and Bader, 1997). The fatigue strength in these S-N diagrams was expressed in terms of %UTS. Cumulative distribution functions were created from the Weibull parameters fit to each stress level (α and β) to calculate the probability P of failure (unreliability) for a given number of cycles N, Eq. (2).

$$P = 1 - e^{-(N/\alpha)^{\beta}} \quad (2)$$

2.5. Statistical analysis

All statistical analysis was completed using SPSS software (IBM, Armonk NY; v24). The effect of stress level and age on failure strain was assessed using an ANOVA, followed by Bonferroni post-hoc tests if significance was detected. The effect of stress-level and age on elongation and dynamic modulus were assessed using a repeated-measures ANOVA, where the within-subject factor was the cyclic creep stage (I, II, III). Differences in the elongation and dynamic modulus at different creep stages were determined using paired t-tests with Bonferroni adjustments for multiple comparisons. The effect of age on the S-N regression lines (slope) was analyzed using hypothesis testing (Taeger and Kuhnt, 2014). For non-parametric analyses, the effect of stress level and age on number of cycles to failure, creep rate, and damage rate was assessed using a medians test, and differences in the number of cycles within each cyclic creep stage were evaluated using a repeated measures sign test. For static failure testing, a MANOVA was used to determine the effect of age on measured mechanical properties (e.g. UTS), and independent t-tests were used to measure differences in static mechanical properties pre- and post-fatigue.

3. Results

3.1. Fatigue life of human meniscus

An S-N diagram (fatigue curve) for human meniscus was generated by combining specimens from both the young and older age groups (Fig. 4). This plot shows that half of meniscus specimens will survive for: 100,000 cycles when pulled to 45% of UTS, one million cycles when pulled to 35% of UTS, ten million cycles when pulled to 24% of UTS, and 250 million cycles (exceeds average number of steps a person would take who lives to 80 years old (Berko et al., 2016)) when pulled to 9.3% of UTS. The semi-log line equation used to make these predictions had an excellent fit ($R^2 = 0.98$) to the median cycles to failure at each stress level. Notably, the y-intercept for the semi-log equation is 98.5, very close to a physiological value of 100. A y-intercept of 100 would correctly predict that a specimen would fail after one cycle when loaded to 100% of UTS.

Cumulative distribution functions were generated using the two Weibull parameters fit to each stress level (α and β; Fig. 5) to determine

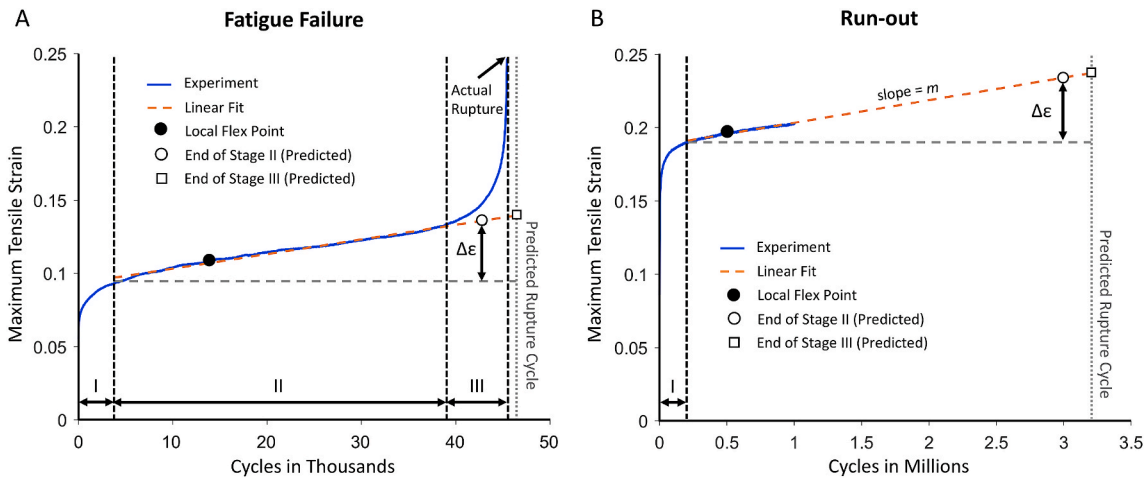

Fig. 3. Analysis of cyclic creep during fatigue testing. A) The cyclic creep curve was split into three characteristic stages: I, II, and III. The creep rate was measured during stage II and the number of cycles to failure occurred at the end of stage III. An algorithm, Eq. (1), was developed to predict the number of cycles to failure by only using experimental data from stage I and II, where Δε represents the mean increase in tensile strain during stage II from all specimens that failed from fatigue. This algorithm could reasonably predict the number of cycles to rupture in specimens that fatigued and B) was applied to all specimens that did not fatigue (run-outs) to predict the number of cycles until rupture.

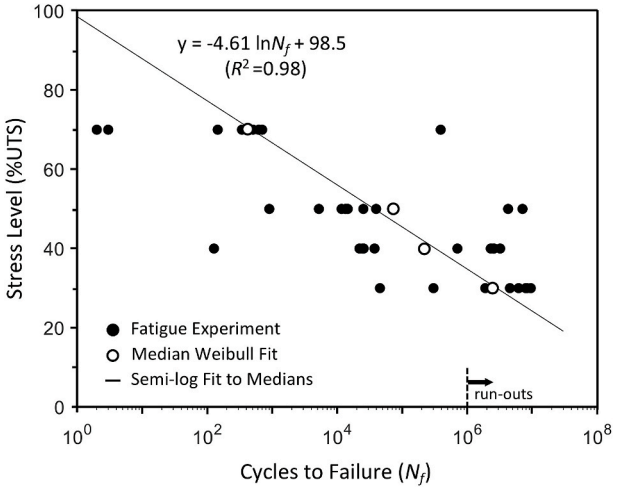

Fig. 4. Fatigue curve for all human meniscus specimens (young and older combined). The median fatigue life at each prescribed stress level was calculated using a Weibull distribution. A semi-log function provided an excellent fit to the median cycles to failure at each stress level ($R^2 = 0.98$). Sample size per stress level = 8.

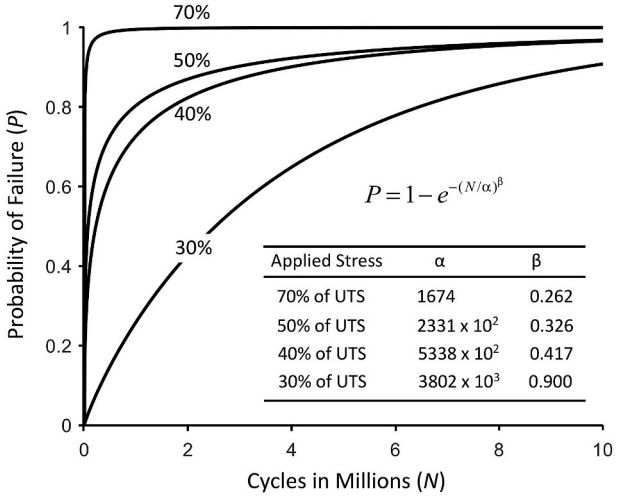

Fig. 5. Cumulative distribution functions for each stress level. The probability of failure P for a given number of cycles N markedly increases when loading meniscus above 30% of UTS.

the probability of failure P for a given number of cycles N, Eq. (2). For example, these functions would estimate that a meniscus specimen loaded in tension for one million cycles at 70%, 50%, 40% or 30% of UTS would have a probability of failure of 100%, 80%, 73%, or 26%, respectively.

The equation for the semi-log fit to the median cycles to failure (Fig. 4) can be reformulated to predict the maximum applied tensile stress (σ_{max})$_{50\%}$, relative to specimen strength (σ_{uts}), that will cause 50% of specimens to fail for a given number of cycles (N). By using the Weibull parameters from each stress level (Fig. 5), similar functions can be created to predict the number of cycles that will cause 5% of specimens to fail (σ_{max})$_{5\%}$ and 95% of specimens to fail (σ_{max})$_{95\%}$. Here is this set of equations for fatigue strength, Eqs. (3)-(5):

$$(\sigma_{max})_{5\%} = \sigma_{uts}\left(-0.026\ln(N_f) + 0.5863\right) \quad 3$$

$$(\sigma_{max})_{50\%} = \sigma_{uts}\left(-0.046\ln(N_f) + 0.9855\right) \quad 4$$

$$(\sigma_{max})_{95\%} = \sigma_{uts}\left(-0.072\ln(N_f) + 1.5518\right) \quad 5$$

These equations can be rearranged to solve for the number of cycles to failure. The following set of fatigue life equations, Eqs. (6)–(8), would then predict the number of cycles that will cause 5% of specimens to fail (N_f)$_{5\%}$, 50% of specimens to fail (N_f)$_{50\%}$, and 95% of specimens to fail (N_f)$_{95\%}$ for a given applied maximum tensile stress (σ_{max}) relative to the specimen's tensile strength (σ_{uts}).

$$(N_f)_{5\%} = e^{-38.46\left(\frac{\sigma_{max}}{\sigma_{uts}} - 0.5863\right)} \quad 6$$

$$(N_f)_{50\%} = e^{-21.74\left(\frac{\sigma_{max}}{\sigma_{uts}} - 0.9855\right)} \quad 7$$

$$(N_f)_{95\%} = e^{-13.89\left(\frac{\sigma_{max}}{\sigma_{uts}} - 1.5518\right)} \quad 8$$

Table 2
Tensile fatigue properties of human meniscus for different age groups and stress levels. Data is reported as either: mean ± standard deviation, or median (interquartile range).

Age	Stress Level (%UTS)	Creep Rate[a] (%/1k cycles)	Damage Rate[a] (%/1k cycles)	Failure Strain (%)
Young	70	9.55 (9.90)	13.0 (15.3)	28.8 ± 7.4
	50	0.63 (0.20)	1.14 (0.57)	29.3 ± 8.3
	40	0.002 (5.83)	0.004 (21.1)	23.4 ± 6.8
	30	0.002 (0.004)	0.003 (0.009)	23.0 ± 5.1
	Total	0.27 (3.17)	0.07 (3.2)	**26.1 ± 7.0**[b]
Older	70	36.3 (23.8)	39.4 (13.0)	18.1 ± 9.4
	50	0.05 (0.93)	0.16 (2.42)	22.5 ± 6.9
	40	0.10 (0.12)	0.27 (0.56)	21.5 ± 3.5
	30	0.001 (0.03)	0.001 (0.025)	22.2 ± 2.3
	Total	0.09 (0.28)	0.07 (0.83)	21.1 ± 5.8
All	70	11.1 (22.2)	22.2 (19.9)	23.5 ± 9.7
	50	0.56 (0.70)	0.66 (1.27)	25.9 ± 7.9
	40	0.04 (0.17)	0.04 (0.60)	22.5 ± 5.1
	30	0.002 (0.005)	0.002 (0.01)	22.6 ± 3.7
	Total	0.09 (1.02)	0.07 (1.5)	23.6 ± 6.8

[a] Data does not include two older 70% tests that failed in less than 5 cycles.
[b] Significantly different than older age group ($p < 0.05$).

3.2. Other fatigue properties of human meniscus

The creep rates, damage rates, and failure strains were calculated for all groups (Table 2). Creep rate significantly increased with each successive stress level ($p = 0.02$). For example, specimens loaded to 70% UTS had median creep rates of 11% per one-thousand cycles, which was over 20 times, 277 times, and 5550 times larger than specimens loaded to 50%, 40%, and 30% UTS, respectively. Similarly, damage rates were greater at higher stress levels ($p = 0.02$). However, stress level did not affect failure strain ($p = 0.74$), where the average failure strain for all specimens was 23.6 ± 6.8%.

Specimen elongation and the number of cycles were calculated at each cyclic creep stage (Table 3). Specimens elongated most during stage I (6.1%), although this elongation was not significantly greater than the other two stages ($p = 0.11$). The stage with the longest duration was stage II, which on average had over 5 times more cycles than stage I and III ($p < 0.001$).

Dynamic modulus decreased during the fatigue test ($p < 0.01$), with significant reductions during each stage of fatigue (Fig. 6). For specimens that failed before one million cycles, the average dynamic modulus decreased by 21% from the start of fatigue testing to the end of stage III, right before rupture ($p < 0.01$) (Fig. 6). For run-out specimens that did not fail before one million cycles, the dynamic modulus increased by 2 ± 7% during fatigue loading, indicating a slight stiffening of the fibrous matrix.

3.3. Effect of age on mechanical properties

Specimen age group affected specimen elongation during fatigue testing, but not other fatigue properties (Table 2). The average tensile failure strain in younger specimens was 26%, and this decreased to 21% in older specimens ($p = 0.035$). When examining specimen elongation at individual stages, young specimens stretched nearly twice the amount of older specimens in stage I ($p = 0.02$), while older specimens stretched nearly twice the amount of young specimens in stage III ($p = 0.04$). This resulted in a significant interaction, where specimen elongation was dependent on specimen age and cyclic creep stage ($p = 0.002$). There was no difference in the number of cycles between young and older

Table 3
Tensile fatigue behavior of human meniscus for different age groups, stress levels, and stages of cyclic creep. Data reported as either: mean ± standard deviation, or median (interquartile range).

Age	Stress Level (%UTS)	Run- outs	Elongation (% increase in specimen length)[a]				Number of Cycles (thousands)[b]			
			Stage I	Stage II	Stage III	All Stages	Stage I	Stage II[c]	Stage III[c]	All Stages[c]
Young	70	0	10.4 ± 5.6	3.6 ± 0.7	2.0 ± 1.5	16.0 ± 7.1	0.17 (13)	0.39 (80)	0.06 (5.0)	0.62 (98)
	50	0	8.0 ± 4.0	7.2 ± 2.6	5.0 ± 3.3	20.2 ± 8.5	1.4 (1.5)	10 (3.8)	1.0 (0.98)	13 (6.3)
	40	3	3.5 ± NA	1.7 ± NA	0.7 ± NA	5.8 ± NA	143 (52)	2277 (718)	143 (52)	2563 (822)
	30	3	4.4 ± NA	1.2 ± NA	4.6 ± NA	10.3 ± NA	102 (103)	1946 (1692)	102 (99)	2150 (1895)
	Total	6	**8.2 ± 4.7**[d]	4.6 ± 2.8	**3.3 ± 2.7**[d]	16.1 ± 8.0	9.4 (142)	47 (2153)	12 (142)	75 (2438)
Older	70	0	5.8 ± 2.0	7.4 ± 2.7	4.7 ± 5.3	17.9 ± 10.0	0.09 (0.01)	0.28 (0.12)	0.06 (0.03)	0.42 (0.08)
	50	2	3.3 ± 2.1	2.9 ± 0.7	4.1 ± 3.6	10.4 ± 6.4	43 (113)	1364 (3660)	43 (113)	1450 (3886)
	40	0	3.2 ± 1.3	4.3 ± 2.0	7.9 ± 3.2	15.4 ± 3.9	2.3 (14)	25 (144)	4.7 (22)	31 (179)
	30	3	3.7 ± NA	3.8 ± NA	11.6 ± NA	19.2 ± NA	172 (185)	5676 (4031)	172 (184)	6243 (4622)
	Total	5	3.9 ± 1.7	4.6 ± 2.3	6.8 ± 3.9	15.3 ± 5.8	4 (111)	32 (3876)	6.4 (110)	43 (4095)
All	70	0	8.9 ± 5.0	4.8 ± 2.4	2.9 ± 3.0	16.6 ± 7.2	0.13 (0.01)	0.38 (0.21)	0.06 (0.06)	0.56 (0.24)
	50	2	6.4 ± 4.0	5.8 ± 3.0	4.7 ± 3.1	16.9 ± 8.8	2.8 (23)	14 (688)	2.6 (23)	19 (735)
	40	3	3.3 ± 1.1	3.8 ± 2.1	6.5 ± 4.2	13.5 ± 5.5	30 (141)	296 (2251)	46 (139)	371 (2531)
	30	6	4.1 ± 0.5	2.5 ± 1.8	8.1 ± 5.0	14.7 ± 6.3	133 (144)	3207 (4767)	133 (139)	3472 (5161)
	Total	11	6.1 ± 4.1	4.6 ± 2.5	5.0 ± 3.7	15.7 ± 6.9	4.3 (137)	32 (2278)	6.4 (137)	43 (2562)

[a] Data excludes run-outs (two older 70% tests that failed in less than 5 cycles were also excluded).
[b] Data includes run-outs (two older 70% tests that failed in less than 5 cycles were excluded).
[c] Cycles predicted for run-outs.
[d] Significantly different than older age group ($p < 0.05$).

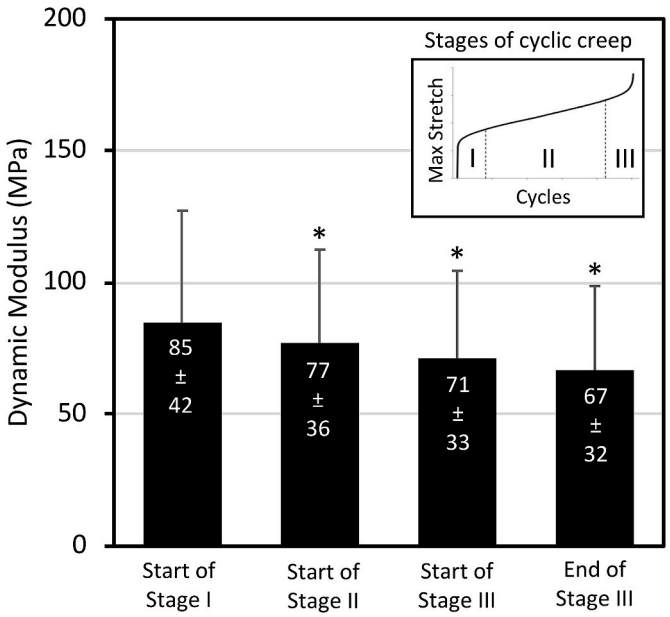

Fig. 6. Dynamic modulus decreased at each stage of creep for specimens that failed during fatigue testing. * = significantly less than all prior time points ($p < 0.01$).

specimens at any stage ($p > 0.9$; Table 3), and age did not have a significant effect on creep rate or damage rate (Table 2).

Fatigue curves (S-N curves) for young and older specimens were plotted to graphically depict fatigue strength at different stress levels (Fig. 7A and B). At first glance, the semi-logarithmic fits seem to indicate that older specimens were more fatigue resistant, as older specimens had a fitted fatigue curve with less slope than young specimens (not significant; $p = 0.30$). However, young specimens had significantly greater (predicted) UTS compared to older specimens ($p = 0.004$), and therefore younger specimens were subjected to on average 78% greater applied tensile stresses than older specimens during fatigue testing ($p = 0.009$). When the semi-log equations for fatigue strength (Fig. 7A and B) are unnormalized by using the average (predicted) UTS values for the specimens, the fatigue curves reveal that young specimens were in fact more fatigue resistant at large stress magnitudes (Fig. 7C), and had comparable fatigue resistance at low stress magnitudes (<2.5 MPa). The young and older fatigue curves converged at a fatigue strength of 2.2 MPa, corresponding to approximately 60 million cycles.

There was a significant effect of age on the static mechanical properties measured during monotonic testing to failure (single pull to failure). Most of the measured static mechanical properties were significantly reduced in older specimens (Table 4).

3.4. Effect of fatigue testing on static mechanical properties

Fatigue testing had a significant effect on the static mechanical properties of meniscus. Specimens that were subjected to one million cycles of loading and then monotonically pulled to failure (i.e. the run-outs) had linear modulus, UTS, and ultimate strain values that were 81% ($p = 0.004$), 54% ($p = 0.026$), and 41% ($p < 0.001$) greater than specimens that were not fatigued prior to monotonic pull to failure testing (Fig. 8).

4. Discussion

The primary objective of this study was to characterize the fatigue strength and endurance limit of human meniscus. These properties are critical to the description and prevention of fatigue failures in engineered structures (Schijve, 2003), yet are not reported for meniscus, a frequently injured tissue that is exposed to large and repeated tensile loads. For visualization, various fatigue strengths calculated in this study can be marked on a stress-strain curve (Fig. 9) that was created using averaged data from monotonic tensile tests of human meniscus (Table 4). This plot shows that the meniscus can withstand one million loading cycles at 35% of UTS (3.7 MPa), and becomes rapidly more susceptible to fatigue near the yield point, which marks the deformation where damage accumulation begins to soften the tissue. If we estimate that 250 million cycles will exceed the number of gait cycles an 80 year old is expected to experience in their lifetime (Berko et al., 2016), we can calculate the endurance limit for human meniscus to be approximately 10% of UTS, or roughly 1.0 MPa based on our average UTS values for human meniscus (Table 4; UTS = 10.6 ± 8.4 MPa). This endurance limit occurs in the toe region, where the crimped collagen fibers are being gradually recruited prior to their collective straightening at the transition point (Fig. 9). Keep in mind that our experiments did not account for viscoelastic recovery that may occur during extended rest periods (e.g. sleep) (Crisco et al., 1997). Viscoelastic recovery could protect against fatigue failure by slowing the rate of cyclic creep. Moreover, our experiments do not account for cellular remodeling of the extracellular matrix. While there is evidence that collagen remodeling does not occur in adult human meniscus (Våben et al., 2020), the mechanobiological response of adult meniscus is not fully known. For these reasons, the fatigue strength and endurance limit reported in this study should be viewed as conservative estimates.

Results from this study give insight into the relative risk of daily

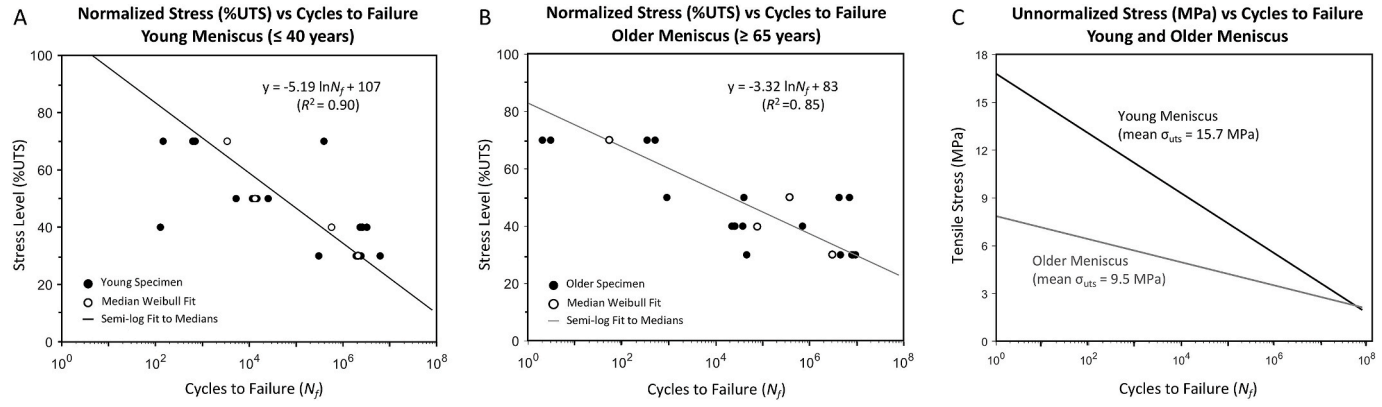

Fig. 7. Fatigue curves for both age groups. Semi-log functions provided good fits to the median cycles to failure at each stress level for A) young specimens ($R^2 = 0.90$) and B) older specimens ($R^2 = 0.85$). Here, stress level is calculated by normalizing the applied maximum tensile stress to the specimen-specific tensile strength (σ_{uts}). C) Alternatively, stress level can be converted to MPa using the average UTS predicted for all young and older specimens. This plot shows that while young specimens can withstand more loading cycles at high stresses, older specimens have comparable resistance to fatigue failure at lower stresses.

Table 4
Tensile static properties of human medial meniscus when monotonically loaded longitudinal to the circumferential fiber direction (single pull to failure). Specimens were harvested from the same menisci used for fatigue testing (number of specimens for each age group: young = 8, older = 8, all = 16).

Age Group	Linear Modulus (MPa)	Transition Stress (MPa)	Transition Strain (%)[b]	Yield Stress (MPa)	Yield Strain (%)[b]	Ultimate Stress (MPa)	Ultimate Strain (%)[b]
Young (<40 yrs)	101.7 ± 71.6	2.9 ± 2.4	5.6 ± 1.9	6.8 ± 5.5	8.9 ± 2.5	14.9 ± 9.9	19.6 ± 3.6
Older (>65 yrs)	47.5 ± 12.0	1.0 ± 0.3[a]	3.9 ± 0.6[a]	2.4 ± 0.8[a]	6.6 ± 0.9[a]	6.3 ± 3.3[a]	15.5 ± 4.5
All	74.6 ± 56.9	2.0 ± 1.9	4.8 ± 1.6	4.6 ± 4.4	7.7 ± 2.2	10.6 ± 8.4	17.6 ± 4.5

[a] Significantly less than young age group ($p < 0.05$).
[b] Measured using grip-to-grip strain.

activities to meniscal injury. The type of meniscal injury associated with the tensile loading condition applied in this study is a radial meniscal tear, which causes substantial loss of meniscal function (Mononen et al., 2013). Human walking is estimated to produce average tensile strains of 3.8% (Kolaczek et al., 2016), corresponding to a tensile stress of 1.3 MPa, which is near the estimated 1.0 MPa endurance limit and therefore indicates that walking is a very low-risk activity for a fatigue injury. Our results suggest that a relatively safe loading limit for repetitive strenuous activities is 30% of UTS, where the estimated median life is nearly 3 million cycles (Fig. 5). This is a dramatic decrease from loading at 40% of UTS, near the yield point, where the estimated median life is 200,000 cycles.

A principal finding of this study was that age did not have a measurable effect on tensile fatigue strength, when normalizing to UTS. We had hypothesized that older specimens (>65 years) would have reduced fatigue strength compared to young specimens (<40 years), but our results did not fully support this hypothesis, as we discovered no significant differences in the normalized S-N curves for young and older meniscus (Fig. 7A and B). This suggests that tensile fatigue failure for all ages of adult menisci can be predicted using a single normalized S-N curve (Fig. 4). It's critical to point out that we normalized the S-N curves based on the predicted strength of the tested fatigue specimens, and the young group had specimens with significantly greater predicted tensile strength compared to the older group. If we examine the S-N curve based on applied tensile stress (Fig. 7C), it becomes evident that young specimens were much more resistant to large fatigue stresses. For example, on average, young specimens withstood approximately one million cycles at 6 MPa of tensile stress, while older specimens failed at this same stress magnitude after approximately one thousand cycles (Fig. 7C). However, at lower magnitude fatigue stresses (<2.5 MPa), young and older meniscus specimens had similar resistance to fatigue failure (Fig. 7C). If we consider that the older specimens (average age = 72 years) experienced on average 40 more years of activity than the younger specimens (average age = 31 years), yet have similar fatigue resistance at low magnitude stresses, we can infer that viscoelastic recovery during extended rest periods is an effective mechanism to protect soft tissue from low-stress fatigue failures.

Aging was found to have an effect on extensibility during fatigue testing, as older specimens elongated one-fifth less than young specimens prior to failure. Interestingly, older specimens experienced less primary cyclic creep (stage I) and more tertiary cyclic creep (stage III) than younger specimens (Table 3). An overall reduction in extensibility with aging has also been reported in our group's previous study that used digital image correlation to measure localized strains in the tear region during single pull to failure experiments (Nesbitt et al., 2021). Age-dependent reductions in extensibility may be due to cumulative damage (Zitnay et al., 2017) or changes in extracellular matrix composition and organization as we age.

The shape of the fatigue curve provided two other interesting observations. First, the fatigue response was logarithmic, where a semi-log function (natural log) gave excellent fits to the median cycles to failure at each stress level, and the fitted y-intercept correctly predicted that the application of stress equal to the tissue's ultimate tensile strength will cause failure in one cycle (Fig. 4). The logarithmic nature of soft tissue fatigue has also been observed in bovine meniscus (Creechley et al., 2017), and human tendon (Schechtman and Bader, 1997). Second, the tensile fatigue strength of human meniscus at one million cycles (~30% of UTS) is relatively low compared to bone and unidirectional carbon fiber composites (~50% of UTS) (Zioupos et al., 2008; Alam et al., 2019); but is similar to several types of thermoplastic polymers (Chandran, 2016; Mura et al., 2018) and woven glass fiber composites (Kumagai et al., 2005; Stevens, 1964). This places the meniscus among

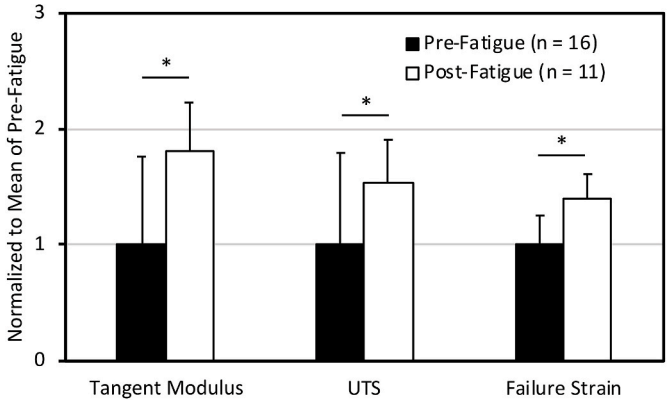

Fig. 8. One million cycles of fatigue testing resulted in run-out specimens ("post-fatigue") with greater modulus, UTS, and failure strain than specimens that were not fatigue tested ("pre-fatigue"). * = significant difference ($p < 0.05$).

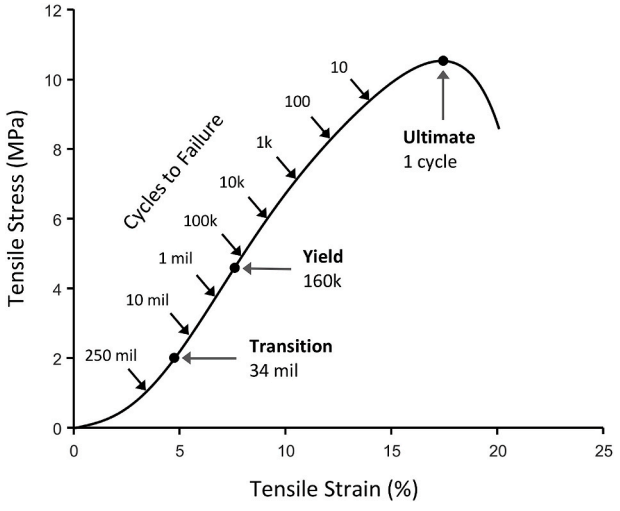

Fig. 9. Fatigue life has been superimposed on a representative stress-strain curve for meniscus. The curve is built using average stress values from uniaxial pull to failure tests of human medial meniscus (Table 4). Here, cycles to failure represents a 50% probability of failure. The endurance limit (250 million cycles) is inside the toe region, suggesting that stresses below the transition point are relatively fatigue resistant. At yield stress, where damage causes the slope of the curve to begin decreasing, the meniscus is predicted to fail after 160,000 cycles (160k).

materials with relatively poor fatigue resistance, and it indicates that mathematical theories used to describe and predict fatigue in polymers and woven fiber composites (Quaresimin et al., 2010) may be applicable to soft fibrous tissue.

Fatigue loading had both a damaging and a strengthening effect. In specimens that failed during fatigue tests, the dynamic modulus was reduced by 21 ± 9% (Fig. 6). This suggests that a damage value of 0.20 may be an appropriate threshold for fatigue failure. In specimens that did not fail during fatigue testing (run-outs), and were then pulled to failure, we observed an increase in static mechanical properties (modulus, UTS, and failure strain) (Fig. 8). Interestingly, these run-out specimens had an overall slight increase in dynamic modulus of 2 ± 8%, indicating that negligible damage occurred during fatigue testing. Together, this suggests that repeated loading below a damage threshold gradually aligns the collagen network, which in turn increases structural stiffness and strength as the tissue elongates.

The calculation of safe loading limits is paramount in mechanical analysis and design, and this study has developed equations to facilitate this analysis for meniscus. The unreliability equations (Fig. 5) can estimate the risk of failure when meniscus is stretched to 70%, 50%, 40% and 30% of UTS for a specified number of cycles. We developed these equations by testing multiple specimens at individual stress levels, per international standards for uniaxial fatigue testing of polymers (ASTM, 2017). The unreliability equations were then used to determine the number of cycles to failure associated with a 5%, 50%, and 95% risk of failure for any specified stress, Eqs. (6)–(8). These formulations could be invaluable to research groups that want to interpret the physical significance of meniscus stresses determined using sensors (e.g. strain gauges), imaging techniques (e.g. MRI), or computational tools (e.g. finite elements). Our formulas can give guidance on safe stress limits, and can provide insight into how changes in stress states due to pathology, anatomical variation, movement, or clinical intervention can impact the risk of fatigue injury.

In order to estimate the fatigue life (N_f) for specimens that did not fail after one million cycles (run-outs), a novel algorithm was developed, Eq. (1). This algorithm used experimental data from stage I and II of cyclic creep to predict the end of stage III (specimen rupture). We developed the algorithm by observing that stage II of the cyclic creep curve was linear over a range of stress amplitudes (1.5–18 MPa) and had a relatively consistent change in strain in stage II between all specimens (4.6 ± 2.5%). When applying this algorithm to specimens that failed before one million cycles, we successfully predicted the number of cycles to failure with a median accuracy of 18%, giving us reasonable confidence in our fatigue life predictions for the run-outs (Fig. 4). Nevertheless, it is possible that cyclic creep would start to non-linearly plateau at very low stress levels and no longer match our model assumption. This possibility reinforces our earlier statement that our endurance limit results should be considered a conservative estimate. This novel and simple algorithm for predicting fatigue life may be useful to other research groups that have run-outs in their fatigue experiments (Riemenschneider et al., 2019).

The mechanical properties measured in the present study can be compared to published work. While no study has measured the tensile fatigue strength of human meniscus, our group did previously measure fatigue in bovine meniscus by measuring cycles to failure (up to 20,000 cycles) at stress levels between 60 and 90% of UTS (Creechley et al., 2017), and the results are strikingly similar to our present study. For example, the tensile fatigue strength at one million cycles was estimated to be 40% of UTS for bovine meniscus, compared to 35% for human meniscus; and the tensile fatigue strength at 250 million cycles was estimated to be 11% of UTS for bovine meniscus, compared to 9% for human meniscus. These similarities would indicate that bovine meniscus is an appropriate animal model to investigate in vitro fatigue and overuse injuries. Our results are less aligned with a prior fatigue study on human extensor digitorum longus tendon (Schechtman and Bader, 1997), as our meniscus fatigue strength was nearly 3x greater than tendon fatigue strength at one million cycles, when normalizing to UTS. One potential explanation for this difference from an evolutionary perspective is that meniscus does not have tendon's regenerative capacity (Dyment and Galloway, 2015), and therefore the fibrocartilaginous extracellular matrix of meniscus may have developed compositional and organizational attributes better suited for withstanding repetitive load. Our static mechanical properties for medial meniscus (Table 4) are generally comparable to a study we previously published on human lateral meniscus (Nesbitt et al., 2021). The greatest disparity in static mechanical properties between the two studies was that the older medial specimens in the present study had nearly 35–50% less tensile strength and stiffness than the older lateral meniscus. We also measured approximately one-sixth more elongation to failure (at UTS) in the present study for both young and older specimens. A likely reason for these differences in elongation is tissue hydration. Nesbitt et al. conducted monotonic mechanical tests in open air, while the present study was conducted in a heated saline bath.

This study had limitations. Fatigue experiments were conducted on the medial meniscus, and fatigue properties may be different in the lateral meniscus. Similar to our previous fatigue study with bovine meniscus (Creechley et al., 2017), we used a preconditioning strain of 8% to measure linear modulus and predict UTS prior to fatigue testing. This preconditioning strain is near the yield strain, and therefore it's possible that some damage occurred during preconditioning that would affect fatigue behavior. However, the present study has shown that specimens can be repeatedly loaded at 8% grip-to-grip strain for over 100,000 cycles (Fig. 9), and therefore any damage that occurred from twenty preconditioning cycles is likely minimal. Results from this study are specific to tensile-tensile fatigue loads, and we did not characterize the sensitivity of the fatigue behavior to variable loading regimes. Finally, the meniscus is an anisotropic material, and the tensile fatigue properties reported in this study only represent the longitudinal fatigue behavior when loading parallel to the circumferential fiber direction. Our prior study with bovine meniscus would suggest that the human meniscus would be relatively more fatigue resistant when loaded transverse to the circumferential fibers, after normalizing for direction dependent tensile strength (Creechley et al., 2017).

In conclusion, this study has characterized the fatigue behavior of human medial meniscus under tensile loading. Mechanical properties and probabilistic functions have been provided that can help spur advancements in the prevention and treatment of soft tissue injuries caused by repetitive loading.

Declaration of competing interest

The authors declare that they have no known competing financial interests or personal relationships that could have appeared to influence the work reported in this paper.

Acknowledgements

This project was supported by the National Science Foundation under grant no. 1554353 and the National Institute of General Medical Sciences under grant no. P20GM109095. We also are grateful to the Engineering Innovation Studio at Boise State University for helping 3D print the tissue punches.

Appendix A. Supplementary data

Supplementary data to this article can be found online at https://doi.org/10.1016/j.jmbbm.2021.105057.

References

Alam, P., Mamalis, D., Robert, C., Floreani, C., Ó Brádaigh, C.M., 2019. The fatigue of carbon fibre reinforced plastics - a review. Compos. B Eng. 166, 555–579. https://doi.org/10.1016/j.compositesb.2019.02.016.

ASTM, 2017. Test method for uniaxial fatigue properties of plastics. ASTM Int. https://doi.org/10.1520/D7791-17.

Berko, J., Goetzel, R.Z., Roemer, E.C., Kent, K., Marchibroda, J., 2016. Results from the bipartisan policy center's CEO council physical activity challenge to American business. J. Occup. Environ. Med. 58, 1239–1244. https://doi.org/10.1097/JOM.0000000000000897.

Budynas, R., Nisbett, K., 2014. Shigley's Mechanical Engineering Design, tenth ed. McGraw-Hill Education, New York, NY.

Bursac, P., York, A., Kuznia, P., Brown, L.M., Arnoczky, S.P., 2009. Influence of donor age on the biomechanical and biochemical properties of human meniscal allografts. Am. J. Sports Med. 37, 884–889. https://doi.org/10.1177/0363546508330140.

Camanho, G.L., Hernandez, A.J., Bitar, A.C., Demange, M.K., Camanho, L.F., 2006. Results of meniscectomy for treatment of isolated meniscal injuries: correlation between results and etiology of injury. Clinics 61, 133–138. https://doi.org/10.1590/s1807-59322006000200008.

Chandran, K.S.R., 2016. Mechanical fatigue of polymers: a new approach to characterize the SN behavior on the basis of macroscopic crack growth mechanism. Polymer 91, 222–238. https://doi.org/10.1016/j.polymer.2016.03.058.

Creechley, J.J., Krentz, M.E., Lujan, T.J., 2017. Fatigue life of bovine meniscus under longitudinal and transverse tensile loading. J. Mech. Behav. Biomed. Mater. 69, 185–192. https://doi.org/10.1016/j.jmbbm.2016.12.020.

Crisco, J.J., Chelikani, S., Brown, R.K., Wolfe, S.W., 1997. The effects of exercise on ligamentous stiffness in the wrist. J. Hand Surg. Am. 22, 44–48. https://doi.org/10.1016/S0363-5023(05)80178-9.

Ding, C., Martel-Pelletier, J., Pelletier, J.-P., Abram, F., Raynauld, J.-P., Cicuttini, F., Jones, G., 2007. Meniscal tear as an osteoarthritis risk factor in a largely non-osteoarthritic cohort: a cross-sectional study. J. Rheumatol. 34, 776–784.

Dyment, N.A., Galloway, J.L., 2015. Regenerative biology of tendon: mechanisms for renewal and repair. Curr. Mol. Biol. Rep. 1, 124–131. https://doi.org/10.1007/s40610-015-0021-3.

Englund, M., Guermazi, A., Gale, D., Hunter, D.J., Aliabadi, P., Clancy, M., Felson, D.T., 2008. Incidental meniscal findings on knee MRI in middle-aged and elderly persons. N. Engl. J. Med. 359, 1108–1115. https://doi.org/10.1056/NEJMoa0800777.

Fatemi, A., 2000. Metal Fatigue in Engineering, second ed. Wiley-Interscience, New York.

Fischenich, K.M., Lewis, J., Kindsfater, K.A., Bailey, T.S., Haut Donahue, T.L., 2015. Effects of degeneration on the compressive and tensile properties of human meniscus. J. Biomech. https://doi.org/10.1016/j.jbiomech.2015.02.042.

Fox, A.J.S., Bedi, A., Rodeo, S.A., 2012. The basic science of human knee menisci: structure, composition, and function. Sport Health 4, 340–351. https://doi.org/10.1177/1941738111429419.

Harris, B. (Ed.), 2003. Fatigue in Composite, first ed. CRC Press, Boca Raton.

Kempson, G.E., 1982. Relationship between the tensile properties of articular cartilage from the human knee and age. Ann. Rheum. Dis. 41, 508–511. https://doi.org/10.1136/ard.41.5.508.

Kolaczek, S., Hewison, C., Caterine, S., Ragbar, M.X., Getgood, A., Gordon, K.D., 2016. Analysis of 3D strain in the human medial meniscus. J. Mech. Behav. Biomed. Mater. 63, 470–475. https://doi.org/10.1016/j.jmbbm.2016.06.001.

Kumagai, S., Shindo, Y., Inamoto, A., 2005. Tension–tension fatigue behavior of GFRP woven laminates at low temperatures. Cryogenics 45, 123–128. https://doi.org/10.1016/j.cryogenics.2004.06.006.

Loeser, R.F., 2010. Age-related changes in the musculoskeletal system and the development of osteoarthritis. Clin. Geriatr. Med. 26, 371–386. https://doi.org/10.1016/j.cger.2010.03.002.

Majewski, M., Susanne, H., Klaus, S., 2006. Epidemiology of athletic knee injuries: a 10-year study. Knee 13, 184–188. https://doi.org/10.1016/j.knee.2006.01.005.

McKeen, L., 2009. Fatigue and Tribological Properties of Plastics and Elastomers, second ed. William Andrew.

Mononen, M.E., Jurvelin, J.S., Korhonen, R.K., 2013. Effects of radial tears and partial meniscectomy of lateral meniscus on the knee joint mechanics during the stance phase of the gait cycle–A 3D finite element study. J. Orthop. Res. 31, 1208–1217. https://doi.org/10.1002/jor.22358.

Morrill, E.E., Tulepbergenov, A.N., Stender, C.J., Lamichhane, R., Brown, R.J., Lujan, T. J., 2016. A validated software application to measure fiber organization in soft tissue. Biomech. Model. Mechanobiol. 15, 1467–1478. https://doi.org/10.1007/s10237-016-0776-3.

Mura, A., Ricci, A., Canavese, G., 2018. Investigation of fatigue behavior of ABS and PC-ABS polymers at different temperatures. Materials 11, 1818. https://doi.org/10.3390/ma11101818.

Nelson, S.J., Creechley, J.J., Wale, M.E., Lujan, T.J., 2020. Print-A-punch: a 3D printed device to cut dumbbell-shaped specimens from soft tissue for tensile testing. J. Biomech. 112, 110011 https://doi.org/10.1016/j.jbiomech.2020.110011.

Nesbitt, D.Q., Siegel, D.N., Nelson, S.J., Lujan, T.J., 2021. Effect of age on the failure properties of human meniscus: high-speed strain mapping of tissue tears. J. Biomech. 115, 110126 https://doi.org/10.1016/j.jbiomech.2020.110126.

Quaresimin, M., Talreja, R., Susmel, L., 2010. Fatigue behaviour and life assessment of composite laminates under multiaxial loadings. Int. J. Fatig. 32, 2–16.

Riemenschneider, P.E., Rose, M.D., Giordani, M., McNary, S.M., 2019. Compressive fatigue and endurance of juvenile bovine articular cartilage explants. J. Biomech. 95, 109304 https://doi.org/10.1016/j.jbiomech.2019.07.048.

Sadeghi, H., Espino, D.M., Shepherd, D.E.T., 2017. Fatigue strength of bovine articular cartilage-on-bone under three-point bending: the effect of loading frequency. BMC Muscoskel. Disord. 18, 142. https://doi.org/10.1186/s12891-017-1510-8.

Schechtman, H., Bader, D.L., 1997. In vitro fatigue of human tendons. J. Biomech. 30, 829–835. https://doi.org/10.1016/s0021-9290(97)00033-x.

Schijve, J., 2003. Fatigue of structures and materials in the 20th century and the state of the art. Int. J. Fatig. 25, 679–702. https://doi.org/10.1016/S0142-1123(03)00051-3.

Scholze, M., Singh, A., Lozano, P.F., Ondruschka, B., Ramezani, M., Werner, M., Hammer, N., 2018. Utilization of 3D printing technology to facilitate and standardize soft tissue testing. Sci. Rep. 8, 11340 https://doi.org/10.1038/s41598-018-29583-4.

Shepherd, J.H., Screen, H.R.C., 2013. Fatigue loading of tendon. Int. J. Exp. Pathol. 94, 260–270. https://doi.org/10.1111/iep.12037.

Stevens, G.H., 1964. Fatigue Strength of Phenolic Laminates from 1 to 10 Million Cycles of Repeated Load. U.S. Department of Agriculture, Forest Service, Forest Products Laboratory.

Stocker, B.D., Nyland, J.A., Caborn, D.N., Sternes, R., Ray, J.M., 1997. Results of the Kentucky high school football knee injury survey. J. Ky. Med. Assoc. 95, 458–464.

Taeger, D., Kuhnt, S., 2014. Tests in regression analysis. In: Statistical Hypothesis Testing with SAS and R. John Wiley & Sons, Ltd, pp. 239–252. https://doi.org/10.1002/9781118762585.ch16.

Tsujii, A., Nakamura, N., Horibe, S., 2017. Age-related changes in the knee meniscus. Knee 24, 1262–1270. https://doi.org/10.1016/j.knee.2017.08.001.

Våben, C., Heinemeier, K.M., Schjerling, P., Olsen, J., Petersen, M.M., Kjaer, M., Krogsgaard, M.R., 2020. No detectable remodelling in adult human menisci: an analysis based on the C14 bomb pulse. Br. J. Sports Med. 54, 1433–1437. https://doi.org/10.1136/bjsports-2019-101360.

Wale, M.E., Nesbitt, D.Q., Henderson, B.S., Fitzpatrick, C.K., Creechley, J.J., Lujan, T.J., 2021. Applying ASTM standards to tensile tests of musculoskeletal soft tissue: methods to reduce grip failures and promote reproducibility. J. Biomech. Eng. 143 (1), 011011 https://doi.org/10.1115/1.4048646.

Yao, J., Snibbe, J., Maloney, M., Lerner, A.L., 2006. Stresses and strains in the medial meniscus of an ACL deficient knee under anterior loading: a finite element analysis with image-based experimental validation. J. Biomech. Eng. 128, 135–141. https://doi.org/10.1115/1.2132373.

Zioupos, P., Gresle, M., Winwood, K., 2008. Fatigue strength of human cortical bone: age, physical, and material heterogeneity effects. J. Biomed. Mater. Res. 86, 627–636. https://doi.org/10.1002/jbm.a.31576.

Zitnay, J.L., Li, Y., Qin, Z., San, B.H., Depalle, B., Reese, S.P., Buehler, M.J., Yu, S.M., Weiss, J.A., 2017. Molecular level detection and localization of mechanical damage in collagen enabled by collagen hybridizing peptides. Nat. Commun. 8, 14913 https://doi.org/10.1038/ncomms14913.